PAPER

Check for updates

Iron oxide nanoparticle-induced hematopoietic and immunological response in rats

Usha Singh Gaharwar,[a] Sumit Kumar†[b] and Paulraj Rajamani [ID] *[a]

The application and use of iron oxide nanoparticless (IONPs) in the biomedical field are steadily increasing, although it remains uncertain whether IONPs are safe or should be used with caution. In the present study, we investigated the toxicity profile of ultrafine IONPs in rats administered with 7.5, 15 and 30 mg IONPs/kg body wt intravenously once a week for 4 weeks. IONP treatment reduces bone marrow-mononuclear cell proliferation, increases free radical species and DNA damage leading to growth arrest and subsequently apoptosis induction at 15 and 30 mg doses. It also induces apoptosis in undifferentiated hematopoietic stem cells. IONP treatment significantly increased the pro-inflammatory cytokine (Interleukin (IL)-1β, TNF-α, and IL-6) level in serum. The induction in inflammation was likely mediated by splenic M1 macrophages (IL-6 and TNF-α secretion). IONP treatment induces splenocyte apoptosis and alteration in the immune system represented by reduced CD4+/CD8+ ratio and increased B cells. It also reduces innate defense represented by lower natural killer cell cytotoxicity. IONP administration markedly increased lipid peroxidation in the spleen, while the glutathione level was reduced. Similarly, superoxide dismutase activity was increased and catalase activity was reduced in the spleen of IONP-treated rats. At an organ level, IONP treatment did not cause any significant injury or structural alteration in the spleen. Collectively, our results suggest that a high dose of ultrafine IONPs may cause oxidative stress, cell death, and inflammation in a biological system.

1. Introduction

Iron oxide nanoparticles (IONPs) attracts great scientific interest in biomedical fields due to high bio-availability, generation of heat in alternating magnetic field, and localization into specific tissue under the influence of an external magnetic field.[1,2] Due to this unique property, IONPs hold immense potential in biomedical applications such as MRI contrast agent, targeted drug delivery, tissue engineering, tissue repair, thermal ablation therapy, noninvasive *in vivo* cell tracking, and magnetic transfections.[2–5] Recently IONPs, feridex (ferumoxides) and feraheme (ferumoxytol) have been approved by U.S. FDA for MRI, and iron deficiency treatment respectively.[2] Additionally, there are other clinical trials (NCT01411904, NCT01995799, NCT01895829 *etc.* http://clinicaltrials.gov) ongoing exploring the IONPs' utility in imaging, tracking and disease detection.[2] Increasing applications and use of IONPs raise serious public concern about adverse effects of IONPs on human health.[2] A number of studies have described the acute toxicity of the IONPs in animals.[6–9] while other studies reported no apparent signs of toxicity.[3,9,10] Understanding the toxicological profiles of IONPs, a transition metal is

vital to ensure that the products are safe and developed with maximum benefits and minimal risks.[11,12] Multiple *in vitro* studies have demonstrated the IONPs-induced cytotoxicity.[1,2,10,12,13] In contrast, other studies failed to observe any significant toxic effects of IONPs.[14,15] Therefore, it is still an open question whether IONPs is cytotoxic or not. Previously, we reported the IONPs-induced oxidative stress and alteration in blood cell counts in rats.[16] Therefore, present study aimed at to investigate the underlying molecular mechanism of IONPs-induced oxidative and hematopoietic injury.

2. Materials and methods

2.1. Chemical

Dry iron oxide nano-powder (Fe_2O_3) was purchased from Intelligent Materials Pvt. Ltd. (Wilmington, DE, USA). 2,7-Dichlorofluorescin diacetate (DCFH-DA), 5,5-dithiobis-(2-nitrobenzoic acid) (DTNB), 2-thio-barbituric acid, reduced glutathione (GSH), propidium iodide, ethylene diamine tetraacetic acid (EDTA), bovine serum albumin and pyrogallol were purchased from Sigma-Aldrich (St. Louis, MO, USA).

2.2. Nanoparticles characterization

IONPs were characterized as described previously.[1,11,13] IONPs suspension (50 μg ml^{-1} in PBS) was drop casted on a copper grid, air dried at room temperature (25 °C) and then analyzed by

[a]School of Environmental Sciences, Jawaharlal Nehru University, New Delhi, 110067, India. E-mail: paulrajr@yahoo.com; Fax: +91-11-26741586; Tel: +91-11-26704162
[b]School of Life Sciences, Jawaharlal Nehru University, New Delhi, India
† Equal contribution.

transmission electron microscope (JEOL-JEM-2100F, Tokyo, Japan) at accelerating voltage of 200 kV. IONP size was evaluated by SEM (Zeiss EVO40, Zeiss, Germany) operating at 15 kV. The hydrodynamic size distribution was calculated from dynamic light scattering (DLS) method by using a Malvern DLS apparatus (Nano-ZS, Malvern Instruments, Malvern, UK) with a 633 nm He/Ne laser. Briefly, The 50 μg ml^{-1} of freshly prepared Fe_2O_3 NPs suspension in distil water was ultra-sonicated for 10 min and it was further diluted thereafter sonication then sample was transferred to a square cuvette for DLS measurements.

2.3. Animals

Male Wistar rats (7–8 weeks old) were obtained and maintained (T: 23–25 °C, RH 60 ± 5%, 12 h light/dark cycle) at central laboratory animal resources (CLAR), Jawaharlal Nehru University, New Delhi. Rats were fed with standard food pellet and water *ad libitum* as recommended by national institute of nutrition, Hyderabad, India. Animal protocol was approved by Institutional Animal Ethics Committee (IAEC), JNU and guidelines of IAEC and CPCSEA, GoI were followed.

2.4. Iron oxide nanoparticles treatment

Preliminary study was performed to estimate the lethal dose 50 (LD_{50}) using 'staircase method' where five doses (25, 50, 75, 100, 125 mg kg^{-1}) have been selected and only two animals were taken per dose. IONPs intravenously injected in animals and animals were observed for 24 h. Neither death nor clinical sign of toxicity were observed in any group. Therefore, three different doses (7.5, 15 and 30 mg kg^{-1}) were chosen for the study. Twenty-four rats were randomly divided into four groups as follow: (1) saline only; (2) 7.5 mg kg^{-1} IONPs; (3) 15 mg kg^{-1} IONPs; (4) 30 mg kg^{-1} IONPs. Rats were placed inside ventilated perspex container, immobilized and injected with required amount of IONPs suspended in 100 μl saline (0.9% NaCl) from tail vain for once in a week for four weeks. After 72 h from last dose, rats were anesthetized with ketamine (110 mg kg^{-1}) and xylazine (15 mg kg^{-1}), and blood was collected in heparinized tube from tail vain. Following animals were sacrificed by cervical dislocation, washed with 70% ethanol, and spleen, tibias and femurs were removed in aseptic condition.

2.5. Bone marrow mononuclear cells (BM-MNCs) isolation

Bone marrow cells were flushed from femora and tibiae into HBSS containing 2% FCS (Himedia, Mumbai, India) using a 21-gauge needle and syringe. Cells were centrifuged in Histopaque-1083 to isolate BM-MNCs. Cell were cultured in RPMI-1640 containing 10% fetal bovine serum, 2 mm glutamine, 10 μm HEPES buffer, 100 units per ml penicillin, and 100 μg ml^{-1} streptomycin (Himedia, Mumbai, India) at density of 1×10^6 cells per ml.

2.6. Detection of reactive oxygen species (ROS)

BM-MNCs was cultured (4×10^4 cells/200 μl) in 96 well plates and incubated for 12 h. DC-FDA (5 μmol) was added at 30 min prior to end of incubation. Afterward fluorescent emission was

recorded at 512 nm (ext. 490 nm) in ELISA reader (Thermo, MA, USA). Same cells were also visualized under fluorescent microscope (Nikon Eclipse Ti2, Tokyo, Japan).

2.7. Quantitative assay of iron

Cells were isolated, washed twice in PBS, and then incubated with 0.125 μM Calcein-AM (Thermo, MA, USA) for 15 minutes at 37 °C. Cell were separated by flow cytometry (BD FACSARIA-III) and analyzed with FlowJo software (Tree Star, OR, USA).

2.8. Comet assay

DNA damage was measured by alkaline comet assay as described previously.[17] DNA damage was quantified using comet score-IV software (Score Comets, UK).

2.9. Cell cycle assay

Cell cycle assay was performed using propidium iodide as described previously.[18]

2.10. Apoptosis assay

BM-MNCs and splenocytes were cultured for 12 h and then stained with ethidium bromide/acridine orange (200 μg ml^{-1} each in PBS). Cells were visualized under fluorescence microscope (BX51, Olympus, Tokyo, Japan) and differentiated on the basis of emitted florescence (green: live, yellow: apoptotic, red: dead cells). Apoptosis in BM-MNCs was also determined by annexin-V-FITC/propidium iodide staining kit (Strong Biotech, Taiwan) and manufacturer's instructions were followed.

2.11. Mitochondrial membrane potential measurement

Mitochondrial membrane potential was measured by JC-1 dye and CMXRos (Thermo, India) and manufacturer's instructions were followed.

2.12. Hematopoietic stem cells isolation and analysis

For hematopoietic stem cells (LSK cells) isolation, BM-MNCs were incubated with PE-conjugated anti-lineage antibodies (CD45R/B220, Gr-1, CD3e, Ter-119 and Mac-1) and then with anti-CD16/CD32 antibody to block Fc receptors (BD biosciences, CA USA). Following cells were stained with PE-Cy7-anti-Sca-1, APC-anti-c-kit, Alexa Fluor-488 conjugated CD80, CD86 and CD206, separated using FACSCalibur (BD biosciences, CA USA) and analyzed by FlowJo softwere.

2.13. Splenocytes isolation

Splenocytes were prepared as descried previously.[19]

2.14. Macrophage isolation

Splenocytes (2.5×10^6 cells per ml in AIM-V medium, HiMedia, Mumbai, India) were placed in flat-bottom plates and incubated for 2 h (37 °C, 5% CO_2). Afterward, non-adherent cells were removed and remaining RBCs were lysed with RBC lysis buffer. Remaining adherent cells were (~10% of original) cultured in

AIM-V medium, consisting of >95% macrophages as judged by Giemsa's staining.

2.15. Nitric oxide measurement

Macrophages were cultured for 24 h. NO content (nitrite) was measured in culture medium at the end of incubation using kit and manufacturer's instructions were followed (Promega Inc, USA).

2.16. Splenic macrophages

Splenic cells were isolated, stained with CD11b-PE-Cy7, CD11c-APC-Cy7, F4/80-APC and CD-206. The F4/80^{high}CD11b^{high}CD11c and F4/80^{high}CD11b^{high}CD11c and cells were purified by a FACSAria sorter (BD Biosciences, CA, USA).

2.17. Intracellular cytokine staining

Splenocytes were cultured, brefeldin A (10 μg ml^{-1}) was added after 2 h, and cells were incubated further for another 3 h. Following fixation and permeabilization with 2% formaldehyde and 0.5% saponin (Rectapur), intracellular cytokine staining was performed using F4/80-APC, CD11b-PE-Cy7, IL1-APC-Cy7, IL10-APC-Cy7, TNF-α-APC-Cy7 and IL-4-APC-Cy7 (BD biosciences, CA USA). The frequency of IL-1, IL-10, TNF-α or IL-4-positive cells were determined within the F4/80^{high}CD11b^{high} population for splenic macrophages.

2.18. Natural killer cell activity

Various dilutions of effector cell (splenocyte) (2×10^6, 1×10^6, 5×10^5, and 2.5×10^5) were co-cultured with constant number (1×10^4 cells per well) of target cells (YAC-1 cells) in a 96-well plate. The cells were incubated for 6 hours at 37 °C in humidified incubator with 5% CO_2. LDH level in supernatant was measured as described in our previous paper.[17] Controls (target cells + effector cell) and a maximum LDH-release control (target cells + 1% triton) were used to calculate the target cell lysis as follow: (sample OD − spontaneous release) × 100/(maximal release − spontaneous release).

2.19. Cytokines measurements

Serum cytokines (IL-1β, IL-6, IFN-γ, IL-4 and TNF-α) levels were measured by enzyme-linked immunosorbent assay kit and manufacturer's (BD biosciences, CA, USA) instructions were followed.

2.20. Sample preparation for antioxidant enzymes

Spleen was homogenized in sodium phosphate buffer (0.1 M, pH 7.4; 1 : 9 w/v) at 4 °C using a tissue homogenizer. Homogenates was centrifuged at 14 000g for 10 min at 4 °C and supernatant was collected for measurement of lipid peroxidation and antioxidant enzymes activity.

2.21. Lipid peroxidation measurement

Lipid peroxidation was measured in form of thiobarbituric acid reactive substances as described previously.[20]

2.22. Reduced glutathione measurement

Briefly, 0.2 ml of homogenate was mixed with 3 ml of 4% sulphosalicylic acid, centrifuged at 2500 rpm for 15 min and then supernatant was mixed with twice volume of DTNB (10 mM) and PBS.[1] Afterwards, absorbance was recorded at 412 nm with spectrophotometer (Shimadzu UV4100, Japan) and GSH content was expressed as nmol GSH/mg protein.

2.23. Superoxide dismutase activity measurement

Cell lysate equivalent to 50 μg protein was mixed with Triton-X-100 (1%) and incubated for 30 min at 4 °C.[1] Following 1 ml of mixture (0.05 M sodium phosphate buffer pH 8.0, 0.01 M EDTA, 0.27 mM pyrogallol) was added, mixed and absorbance was measured for 5 min at 420 nm with spectrophotometer (Shimadzu UV4100, Japan). Enzyme activity was expressed as U per mg protein.[21]

2.24. Catalase activity

Catalase enzyme was measured as described previously.[22]

2.25. DNA ladder assay

Splenocytes were suspended in lysis buffer (50 mM Tris, pH 7.5, 10 mM EDTA and 0.3% Triton X-100) for 30 min on ice. DNA ladder assay was performed as described previously.[11]

2.26. Histo-pathological analysis

Spleen was dissected out from animals and fixed in 10% formalin. Samples were embedded in paraffin, sectioned, and stained with hematoxylin and eosin and visualized under microscope.
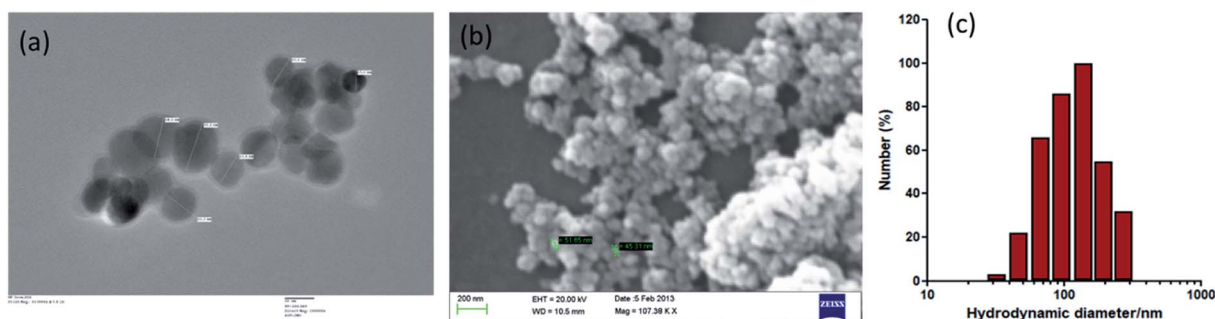

Fig. 1　Characterization of Iron oxide nanoparticles (IONPs). (a) Transmission electron microscope image of IONPs, scale bar: 20 nm; (b) scanning electron microscope image of IONPs. (c) Dynamic light scattering (DLS) histogram for hydrodynamic size distribution of IONPs.

2.27. Statistical analysis

One-way analysis of variance followed by Tukey's multiple comparisons test was employed and $p \leq 0.05$ was considered significant. Results are expressed as means $\pm$ SD. All statistical analyses were done using Graphpad Prism 5 (CA, USA).

3. Results & discussions

3.1. Nanoparticle characterization

IONPs were almost spherical in size as revealed by TEM and SEM (Fig. 1(a and b)). The IONPs size were ~30–35 nm diameters in size as measured by TEM. DLS results show the well distributed and steady state IONPs, with an average size of 138.11 nm (Fig. 1(c)). DLS analysis showed larger size values
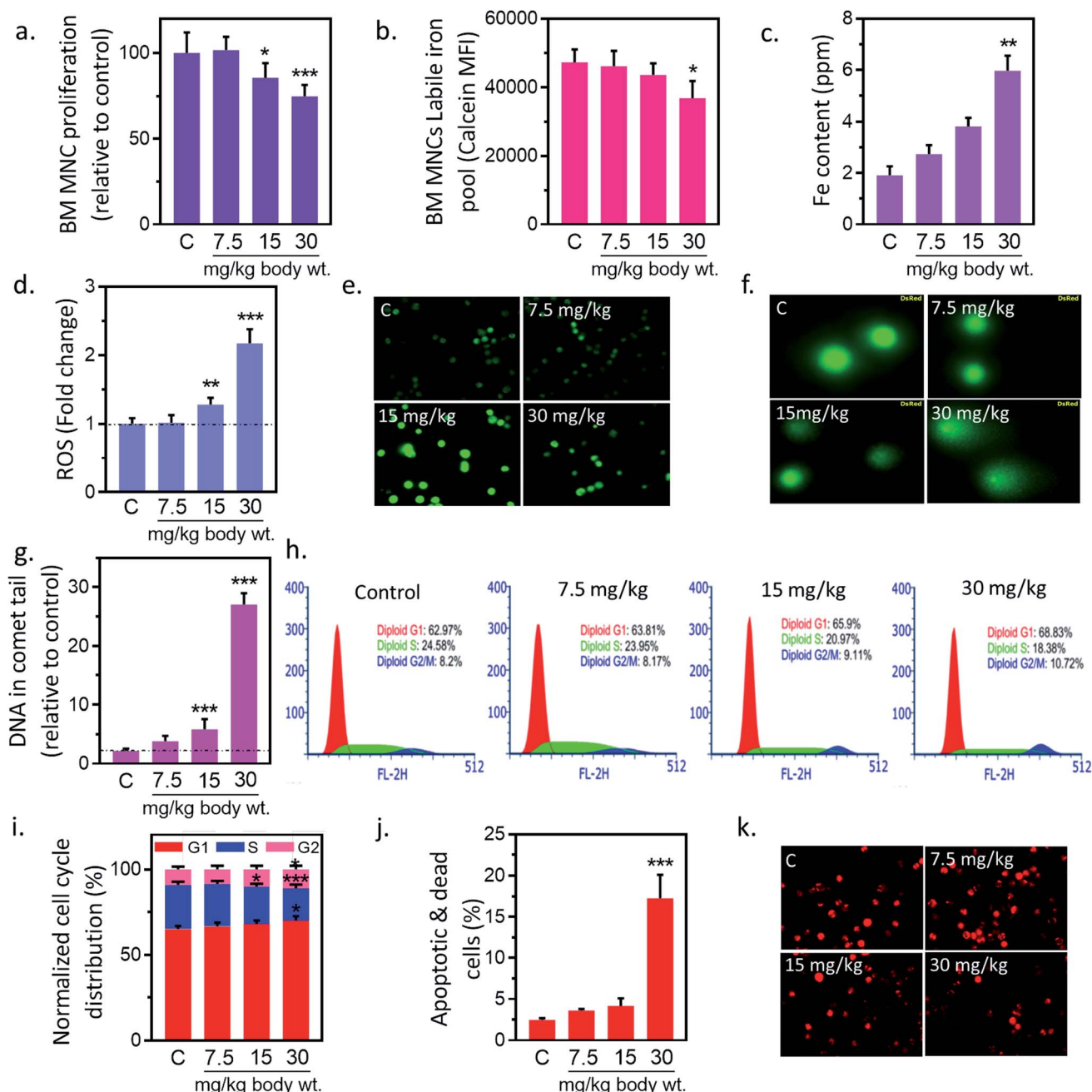
Fig. 2 Iron nanoparticles (IONPs) induce cytotoxic and apoptotic response in bone marrow mononuclear cells (BM-MNCs) of rats. (a) BM-MNCs proliferation, detected by MTT; (b) labile iron pool in BM-MNCs, detected by calcein; (c) iron level in BM-MNCs, detected by coupled plasma atomic emission spectroscopy; (d and e) relative change in BM-MNCs ROS level, detected by DC-FDA; (f and g) BM-MNCs DNA damage, detected by alkaline comet assay; (h and i) activation of cell cycle check point in BM-MNCs (bar represents normalized % distribution of cells in different cell cycle stage); (j) BM-MSCs apoptosis, detected by annexin V propidium iodide; (k) BM-MNCs mitochondrial membrane potential ($\Delta\Psi_m$), measured by Mitotracker CMXROS. Rats were treated with IONPs intravenously for 28 days in a 7 day interval. Each data point represents mean $\pm$ SD. n: 6. *$p < 0.05$; **$p < 0.01$; and ***$p < 0.001$ *versus* saline control.

than NPs measured by TEM that indicates that IONPs formed agglomerates in suspension at higher concentration. EDX analysis revealed that IONPs sample was devoid of any impurity.[16] Similarly, TEM and SEM analyses were performed to determine the morphology of various zerovalent iron composite and obtained spherical shape.[23,24] XRD data revealed that IONPs consists of Fe_2O_3.[16]

3.2. IONPs accumulation in BM-MSCs reduces proliferation

In preliminary study, BM-MNCs proliferation was measured to evaluate the impact of IONPs-induced toxicity since iron is generally transported and accumulated into bone marrow, and spleen *etc.* and utilized in erythropoiesis.[25,26] To understand the impact of IONPs on biological system, rats were administered with increasing doses (7.5, 15, and 30 mg kg^{-1}) of IONPs intravenously once a weak for 4 weeks. IONPs doses were chosen on the basis of past imaging, and tracking studies.[12] BM-MNCs proliferation was measured as preliminary parameter to access the impact of IONPs-induced toxicity. IONPs exposure revealed a significant dose-dependent toxicity in BM-MNCs (Fig. 2(a)). The proliferation was increased by 1.58% ± 0.12 at 7.5 mg per kg dose and reduced by 14.6 ± 1.46 and 25.2% ± 2.15 at 15 and 30 mg per kg ($p < 0.05$) body wt. IONPs respectively (Fig. 2(a)). IONPs exposure revealed a significant dose-dependent inhibition of BMMNCs proliferation. Although multiple studies have documented the role of iron on inhibition of cell proliferation, yet the direct *in vivo* evidence was missing.[12,27] Further we sought to quantify the degree of IONPs accumulation in the form of labile iron pool (LIP) to check whether proliferation reduction indeed a consequence of IONPs. A dose-dependent increase in iron accumulation in BM-MNCs was observed (Fig. 2(b)). IONPs internalization was further confirmed by inductively coupled plasma atomic emission spectroscopy method (Jobin Yvon ULTIMA 2, UK). The cellular iron content was increased by 1.43 ± 0.31, 1.99 ± 0.37 and 3.12-fold ± 0.58 ($p < 0.05$) against untreated control at 7.5, 15, and 30 mg kg^{-1} IONPs (Fig. 2(c)). The high correlation coefficient (0.947) between LIP and proliferation inhibition indicates the direct or indirect role of LIP on proliferation reduction.

3.3. IONPs-induced oxidative stress and DNA damage in BM-MNCs

Ability of IONPs to trigger oxidative stress in BM-MNCs was assessed by measuring the intracellular ROS production. IONPs treatment enhances the ROS level in BM-MNCs by 1.8% ± 0.19, 28.15% ± 2.07, 117.19% ± 11.21 at 7.5, 15 and 30 mg per kg body wt respectively (Fig. 2(d)). However, significant changes were observed at 30 mg per kg dose. IONPs-induced ROS was further confirmed by fluorescence microscopic examination, where DCFDA fluorescence was increased in a dose-dependent manner (Fig. 2(e)). The correlation coefficient between LIP and ROS level was 0.967. Which indicates that increased iron concentration was reason behind ROS generation. IONPs is known to produce toxic $OH^{\cdot}$ radicals through Fenton reaction following its dissolution by lysosomes.[28] However, IONPs is also

reported to reduce cellular H_2O_2 by exhibiting the peroxidase-like activity.[28] Since H_2O_2 has implicated in cell growth regulation, thus author has hypothesized that IONPs stimulate cell proliferation by reducing the H_2O_2. Hence, role of IONPs on induction of ROS and subsequent effect on cell viability and proliferation seems to be interplay of intact and solubilized state.

Elevated ROS can damage DNA and cause lesions in DNA therefore impact of IONPs-induced ROS on DNA was evaluated by Comet assay. IONPs treatment increased the DNA damage in a dose-dependent manner (Fig. 2(f)). The percentage DNA in comet tail was increased from 2.16% ± 0.38 in untreated control to 1.63% ± 0.93, 3.68% ± 1.74, and 24.89% ± 1.91 ($p < 0.05$) at 7.5, 15 and 30 mg per kg body wt (Fig. 2(g)). ROS can generate an oxidative assault on DNA and produce lesions. The damage DNA stalls cell division and mounts an effective DNA repair. Failure to repair DNA results in initiation of cell death pathways.[18] Multiple *in vitro* studies have demonstrated the IONPs-induced DNA damage,[1] however *in vivo* data is scarce. In our study, high doses of IONPs caused DNA damage in BM-MNCs, representing the potential genotoxicity.

3.4. IONPs induced mitochondrial-mediated apoptosis in BM-MNCs

DNA damage can induce apoptosis through activation of cell cycle checkpoints; hence we evaluated the role of IONPs on cell cycle arrest, and apoptosis. Administration of 7.5, 15 and 30 mg kg^{-1} IONPs resulted in reduction of S-phase cells from 24.85% ± 1.71 in untreated control to 23.41% ± 1.58, 20.85% ± 1.75 ($p < 0.05$) and 18.42% ± 2.15 ($p < 0.05$) respectively or increase in G2/M-phase cells from 8.79% ± 1.42 in untreated control to 8.14% ± 1.95, 9.74% ± 1.91 and 10.81% ± 2.01 (Fig. 2(h and i)). Failure to repair damaged DNA following growth arrest can leads to reduction in $\Delta\Psi_m$ and subsequently apoptosis induction. IONPs treatment increase the BM-MNCs apoptosis by 14.7% ± 2.4 ($p < 0.05$) against untreated control at 30 mg per kg body wt (Fig. 2(j)). The reduction in $\Delta\Psi_m$ following IONPs treatment suggests the involvement of intrinsic pathway in IONPs-induced apoptosis (Fig. 2(k)). IONPs-induced DNA damage in BM-MNCs leads to activation of cell cycle check point, reduction of $\Delta\Psi_m$ and subsequently apoptosis induction significantly ($p < 0.05$) at 30 mg per kg dose. Failure to repair damaged DNA leads to collapse of $\Delta\Psi_m$ and apoptosis.[18] However direct role of IONPs on $\Delta\Psi_m$ collapse cannot be rule out as it has shown to inhabit Na^+–K^+ ATPase involved in maintenance of resting potential.[27] Mitochondrial depolarization results in Ca^{2+} ions entry in cells that activates caspase 3-dependent apoptosis pathway through cytochrome c.[29]

3.5. IONPs-induced oxidative stress and apoptosis in LSK cells

Undifferentiated stem cells (LSK cells), a BM-MNCs subpopulation, have long term repopulation ability and contributes to cellularity of mature myeloid and lymphoid cells in peripheral blood.[30] Since cells type is an important parameter in nanoparticles-induced toxicity therefore we checked IONPs

impact on LSK cells to understand the role of IONPs in hematopoietic development and deregulation.[31] Exposure of 7.5, 15 and 30 mg IONPs/kg body wt resulted in enhancement of ROS significantly in LSK cells (Fig. 3(a)). Oxidative stress plays a pivotal role in apoptosis, therefore LSK cell apoptosis was measured to assess the impact of iron-induced oxidative stress. IONPs treatment increases the ROS level and also induces apoptosis in LSK cells. The IONPs induces apoptosis in LSK cells mainly at 15 and 30 mg per kg body wt (Fig. 3(b)). Present findings demonstrate that IONPs induce undifferentiated

hematopoietic stem cells death, and that could be reason for IONPs-induced leukopenia, erythropenia *etc.*[16] IONPs-induce apoptosis in LSK cells either due to ROS or $\Delta\Psi_m$ collapse following IONPs internalization or both.[29,32]

3.6. Measurement of serum cytokines

Inflammation, and immune modulation are two major events in nanoparticles-mediated toxicities.[33] These events can be detected by blood cytokines measurement. Hence, serum cytokine (IL-1β, IL-6, TNF-α) level was measured to further explore
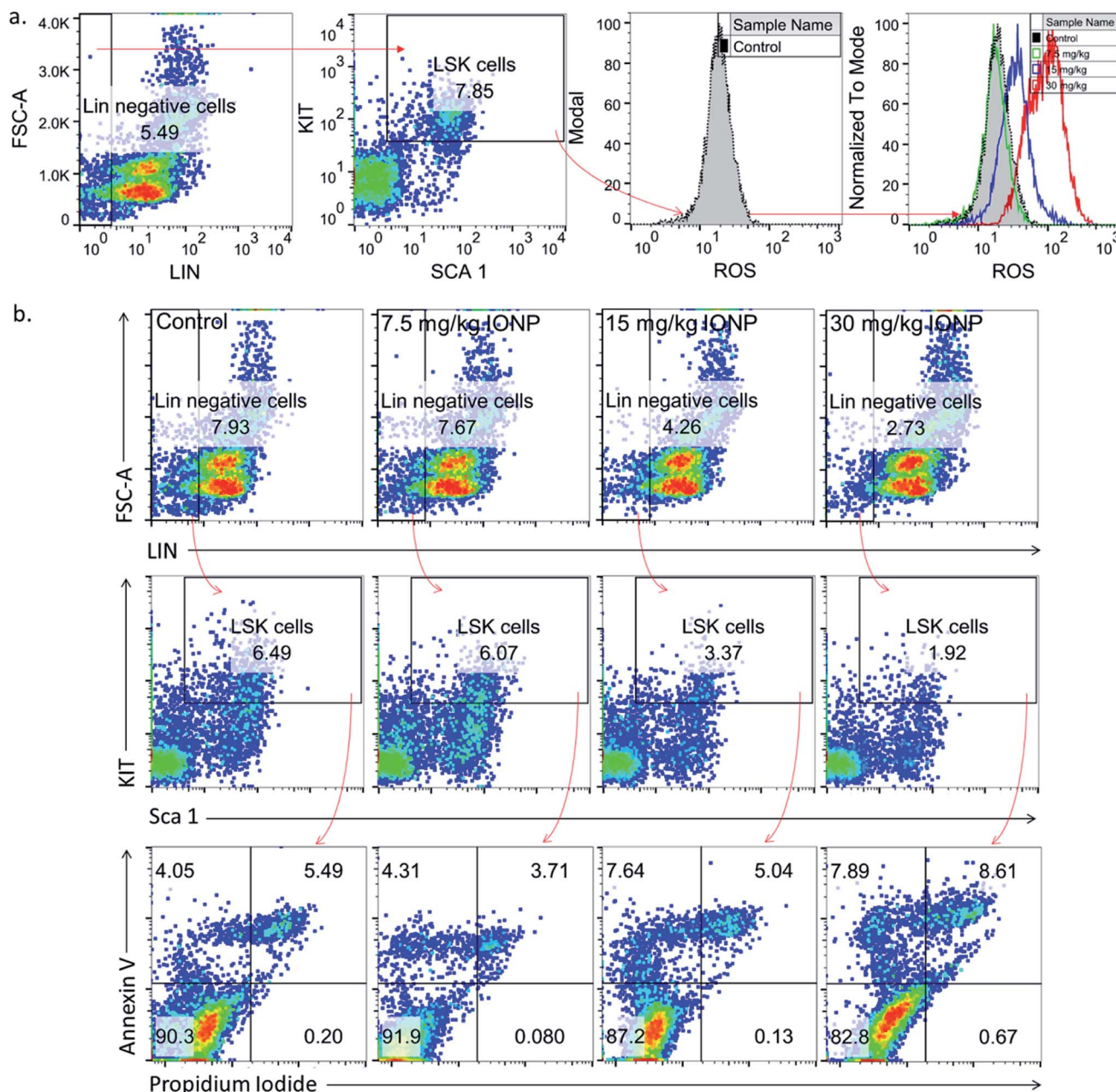

Fig. 3 Iron nanoparticles (IONPs) increase reactive oxygen species in immature bone marrow hematopoietic cells (lineage negative, Sca1 positive, c-kit negative, LSK⁻ cells). (a) Representative gating strategy for LSK⁻ BM populations and ROS level in different groups, measured by DCFDA using flow cytometry; (b) gating strategy for bone marrow LSK cells, LSK⁻ cell apoptosis in different treatment groups. Rats were treated with IONPs intravenously for 28 days in a 7 day interval.

the immune modification by IONPs. IL-1β level was increased from 1.7 ± 0.2 pg ml^{-1} in untreated control to 1.9 ± 0.6, 2.7 ± 0.5 and 5.4 ± 1.1 ($p < 0.05$) pg ml^{-1} at 7.5, 15 and 30 mg kg^{-1} IONPs respectively (Fig. 4(a)). IL-6 level was increased from 3.1 ± 1.0 pg ml^{-1} in untreated control to 4.8 ± 1.7, 21.8 ± 3.4 and 58.1 ± 11.8 ($p < 0.05$) at 7.5, 15 and 30 mg kg^{-1} IONPs respectively (Fig. 4(a)). However, TNF-α level was increased from 1.9 ± 0.3 pg ml^{-1} in untreated control to 1.9 ± 0.4, 3.1 ± 0.2 ($p < 0.05$) and 7.8 ± 1.2 ($p < 0.05$) at 7.5, 15 and 30 mg kg^{-1} IONPs respectively (Fig. 4(a)). In our result, IONPs treatment has shown to increase the blood pro-inflammatory cytokines (IL-1β, IL-6, TNF-α) level, with the strongest response at 30 mg kg^{-1} IONPs dose. Present result indicates that IONPs treatment induces an acute inflammatory response. Our data show that intravenous administration of IONPs in rats increase the level of serum inflammatory cytokines and may be responsible for the inflammation-induced oxidative stress.[34] Production of reactive oxygen species can be induced by nano-materials as nano-materials are able to reach mitochondria and hence may induce inflammatory response in activated macrophages.[35] Microarray analysis revealed that gene responsible for oxidative stress and inflammatory responses undergo for reprogramming in IONPs treated mouse macrophages.[36] We therefore speculate that IONPs-induced ROS activates NF-κB, which subsequently leads to release of pro-inflammatory cytokines.

3.7. IL-4, IFN-γ and NO production in splenocytes

However, the possibility of IONPs recognition as a foreign substance leading to immune cascade activation is also not ruled out. Therefore, we performed immune-phenotyping to elucidate the mechanism of IONPs-induced inflammatory response. Dendritic cell activation through foreign antigen results in activation of Th1, or Th2 immune response.[33] Th1 cells play an important role in generation of inflammatory response, while Th2 induces B cells differentiation and thus promotes humoral immunity. Therefore, we studied Th1 and Th2 cytokines to get insight into mechanism of IONPs-induced inflammatory response. IL-4, IFN-γ and NO level in splenocytes was measured as humoral immune parameters to examine the quantum of immune suppression. IL-4 production was

increased by $3.72\% \pm 0.81$, $36.51\% \pm 6.83$ and $139.01\% \pm 30.27$ ($p < 0.05$) against untreated control at 7.5, 15, and 30 mg kg^{-1} IONPs respectively (Fig. 4(b)), while IFN-γ production was markedly attenuated by 61.7 ($p < 0.05$), and 81.9% ($p < 0.05$) against untreated control at 15, and 30 mg kg^{-1} respectively (Fig. 4(c)). The NO level was found to increase by 0.46 and 1.54-fold ($p < 0.05$) at 15, and 30 mg IONPs dose respectively (Fig. 4(d)). Present result indicates that IONPs treatment promote the dominance of Th1 (IL-4) response over Th2 (IFN-γ) response. Result suggests that IONPs elevate Th1 response (IL-4) and suppress the Th2 (IFN-γ) response. This is in agreement with previous study.[5] IL-4 plays a major role in induction of inflammation by attracting macrophages and then inducing the secretion of IL-6 and TNF-α. In contrast, IFN-γ secreted by Th2 cells responsible for cell proliferation, B cells differentiation, and matrix turnover. Hence, we hypothesized that IONPs induce an inflammatory and oxidative response through spleen M1-macrophages.

3.8. IONPs polarize macrophages into M1 phenotype

Spleen was chosen to study macrophages response as macrophages mainly reside in spleen and recycle iron from ageing erythrocytes. The Th1 immune response promotes macrophage activation, in contrast, Th2 response stimulates antibody production. Hence, we hypothesized that IONPs induce inflammatory response through macrophages. The splenic macrophage proportion was found to increase from 2.67% in untreated control to 2.46, 2.88 and 4.48% at 7.5, 15, and 30 mg kg^{-1} IONPs respectively (Fig. 5(a)).

Further, we phenotypically characterized the macrophage as macrophages function change based on the type of nanoparticles and local environment. Cytokines secreted by M1 macrophages (IL-6, TNF-α, Fig. 5(b and c)) were elevated, while M2 macrophages cytokines (IL-10, IL-4, Fig. 5(e and d)) level were decreased. Our result indicates the IONPs-induced macrophages polarization into M1 phenotype, however the direct evidence of macrophage polarization in spleen was came from checking the M1 (F4/80$^+$CD11c$^+$CD206$^-$) and M2 (F4/80$^+$CD11c$^-$CD206$^+$) macrophage markers. The M1 macrophages were increased from 17.6% in untreated control to

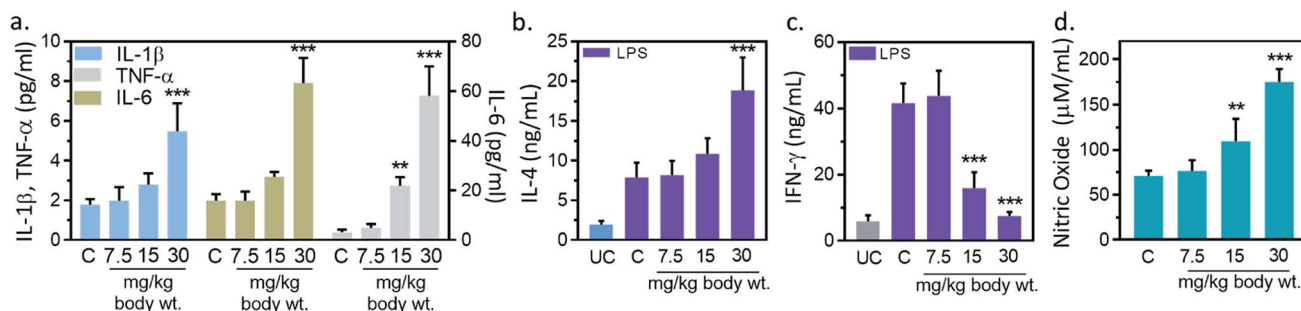**Fig. 4** Iron oxide nanoparticles (IONPs) induce inflammatory response. (a) Blood IL-1β, IL-6 and TNF-α after IONPs treatment; (b) IL-4 production in different treatment groups; (c) IFN-γ production in different treatment groups; (d) nitric oxide production in different treatment groups. All graphs present average ± SEM. *n*: 6. Rats were treated with IONPs intravenously for 28 days in a 7 days interval. **$p < 0.01$; and ***$p < 0.001$ *versus* saline control.
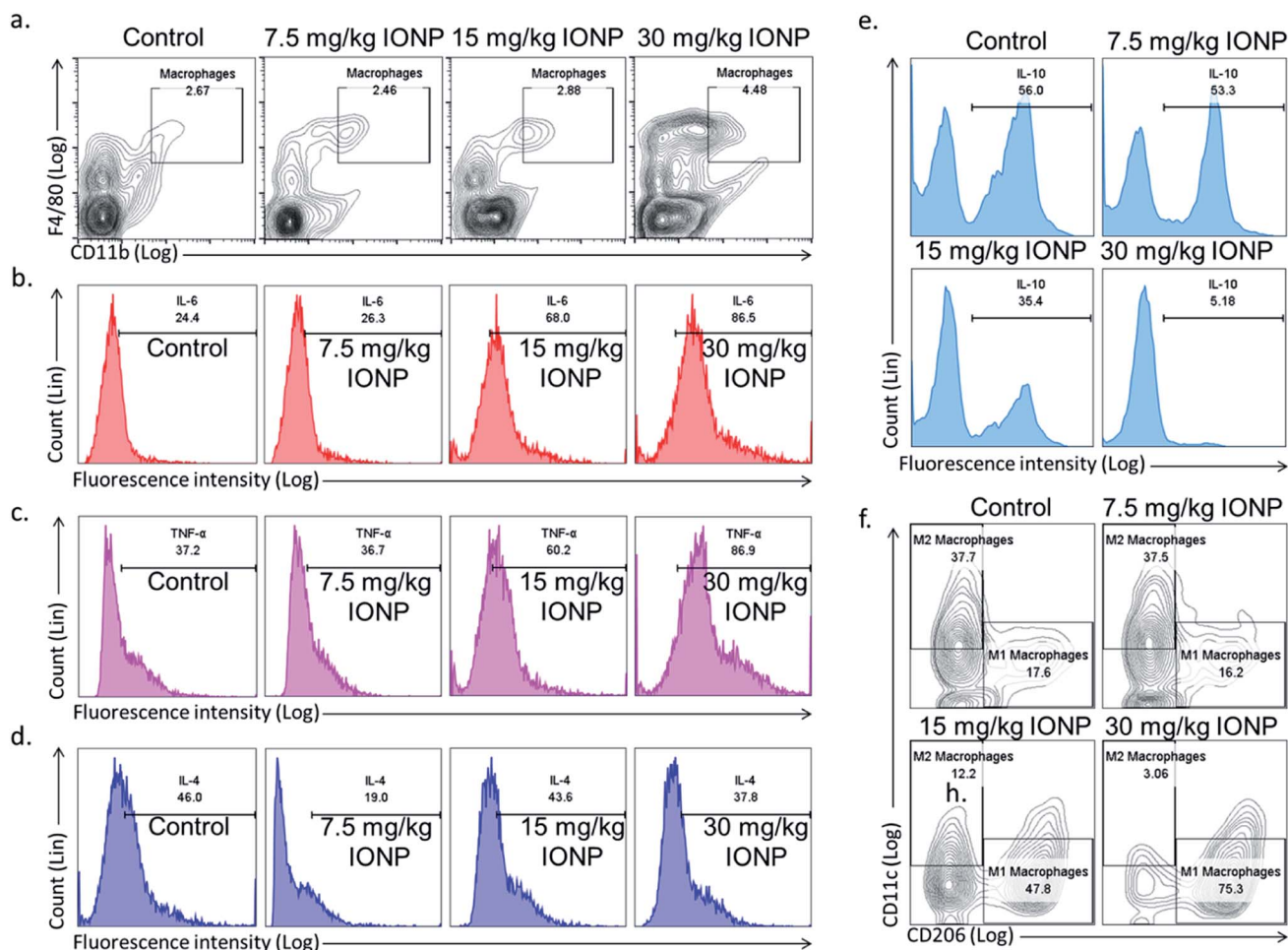
Fig. 5 IONPs induces inflammatory response by macrophage polarization. (a) Characterization of rat splenic macrophages (F4/80^{high}CD11b^{high}) by flow cytometry; (b) IL-6 secretion by macrophages (F4/80^{high}CD11b^{high}); (c) TNF-α secretion by macrophages (F4/80^{high}CD11b^{high}); (d) IL-4 secretion by macrophages (F4/80^{high}CD11b^{high}); (e) IL-10 secretion by macrophages (F4/80^{high}CD11b^{high}); (f) splenic M1 (F4/80^{high}CD11b^{high}CD11c) and M2 macrophages (F4/80^{high}CD11b^{high}CD206) proportion by flow cytometry. Rats were treated with IONPs intravenously for 28 days in a 7 day interval.

16.2, 47.8 and 75.3% at 7.5, 15, and 30 mg kg^{-1} IONPs respectively (Fig. 5(f)). While M2 macrophages were reduced from 37.7% in untreated control to 37.5, 12.2 and 3.06% at 7.5, 15, and 30 mg kg^{-1} IONPs respectively (Fig. 5(f)). Our result demonstrates that IONPs increase the macrophage proportion and also polarized them into M1 phenotype (IL-6 and TNF-α). Accordingly, alternatively activated or M2 macrophage proportion was reduced. Although there are reports showing IONPs role in M1 macrophage polarization in *in vitro* but the direct evidence was lacking.[37] Increased M1 responses are not surprising, as M1 macrophages are known to involve in biological processing of nanoparticles.[38] Macrophages are powerful effector cells of innate immune system, and adopt to different functional programs in response to local microenvironment signals.[11] Iron has shown to sequestered by macrophage, and activates NF-κB.[33] NF-κB further activates the proinflammatory cytokines gene.[39] Our result indicates M1 macrophage as potential player in induction of IONPs-induced inflammatory response.

3.9. IONPs reduce splenocyte's proliferation and induce oxidative stress & apoptosis

Next, we studied the IONPs effect on splenocytes as it represents an important organ in innate and adaptive immune system.[40] Inflammatory response may induce oxidative stress therefore next we check the redox status in splenocytes. IONPs treatment resulted in enhancement of ROS level in splenocytes by 5.8% ± 0.6, 52.4% ± 5.1 and 117.6% ± 11.9 against untreated control at 7.5, 15 and 30 mg per kg dose respectively (Fig. 6(a)). No significant change was observed at 7.5 mg per kg dose. IONPs treatment reduced the splenocyte proliferation by 2.6% ± 0.1 and 15.2% ± 1.6 against untreated control at 15, and 30 mg per kg body wt respectively (Fig. 6(b)). Splenocytes from rat treated with higher dose of IONPs (15 and 30 mg kg^{-1}) showed clear DNA ladder with discontinuous DNA fragments, indicating the apoptosis induction (Fig. 6(c)). No major change was observed at 7.5 mg per kg dose. Collectively, our results suggest that high dose of IONPs induce oxidative stress that results in splenocytes DNA damage. IONPs treatment reduces splenocyte proliferation,
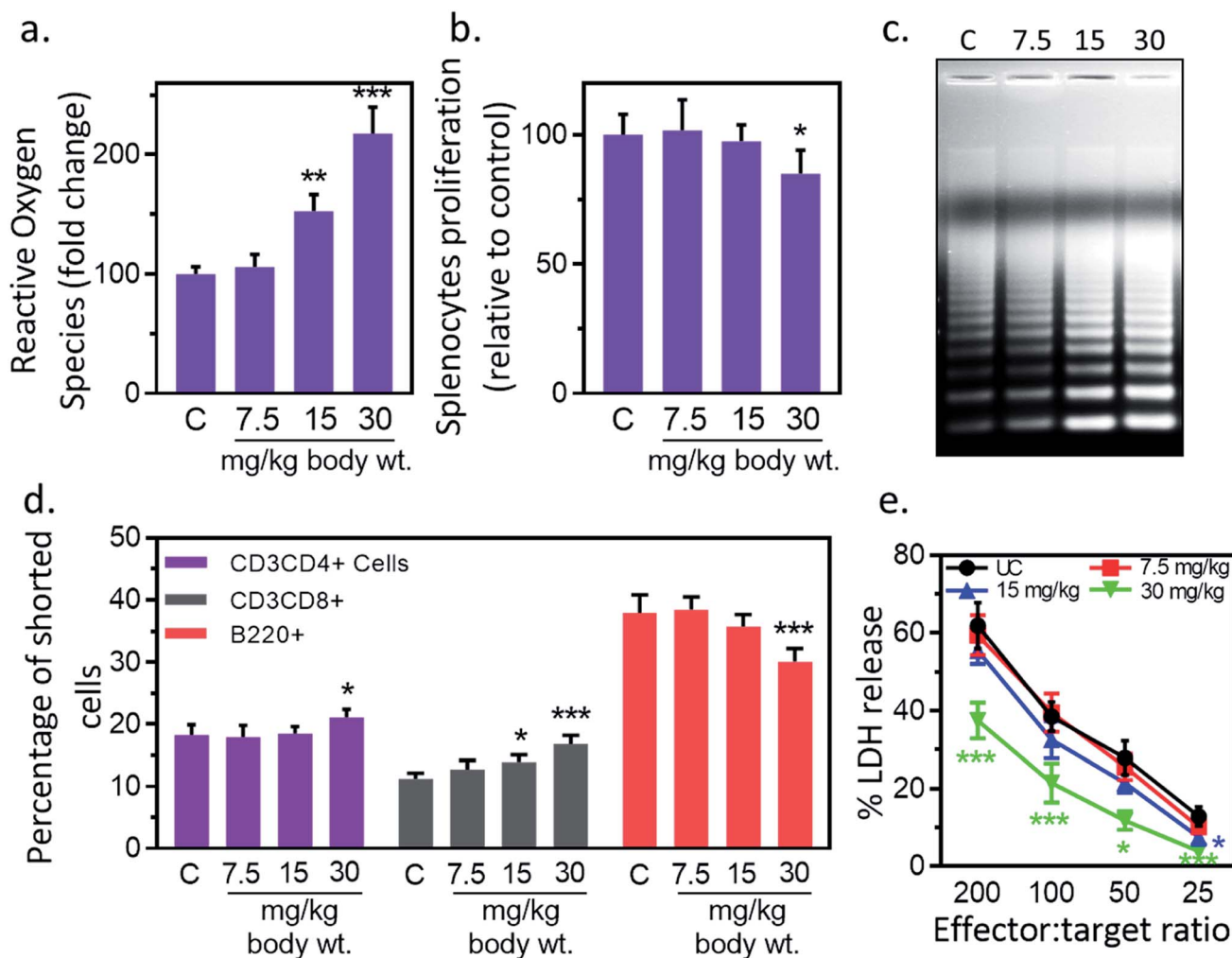
Fig. 6 Iron oxide nanoparticles (IONPs) induce splenocytes apoptotic response. (a) IONPs treatment increases free radicals in splenocytes, measured by DC-FDA assay; (b) IONPs treatment reduces splenocytes proliferation, measured by MTT assay; (c) IONPs treatment increased splenocytes apoptosis, measured by ladder assay; (d) IONPs exposure increased T_c and T_h cells and reduces B cells in spleen; (e) NK cells cytotoxicity against YAC-1 cells. Rats were treated with IONPs intravenously for 28 days in a 7 day interval. Each data point represents mean ± SD. n: 6. *$p < 0.05$; **$p < 0.01$; and ***$p < 0.001$ versus saline control.

induces oxidative stress and apoptosis. Collectively, our results suggest that IONPs induce apoptosis in splenocytes by inducing oxidative stress through M1 macrophage-mediated inflammatory response.

3.10. IONPs treatment alter splenocytes cell distribution

IONPs treatment resulted in reduction of T helper/T cytotoxic cells ratio from 1.4 (18.2% ± 1.7/11.2% ± 0.9) in untreated control to 1.4 (17.9% ± 1.9/12.7% ± 1.5), 1.33 (18.5% ± 1.1/13.9% ± 1.2), and 1.25 (21.1% ± 1.3/16.8% ± 1.4) at 7.5, 15, and 30 mg kg^{-1} respectively (Fig. 6(d)). The number of B220+ was reduced from 37.9% ± 2.9 in untreated control to 38.4% ± 2.1, 35.7% ± 1.9 and 30.1% ± 2.1 at 7.5, 15 and 30 mg kg^{-1} IONPs respectively (Fig. 6(d)). IONPs treatment induces the slight alteration in splenocyte cell distribution. The CD4/CD8 ratio is found to reduce while B cells proportion is found to increase

following IONPs treatment. The reduction in CD4/CD8 ratio indicates the systemic immune suppression by IONPs.[37]

3.11. IONPs treatment reduces NK cell cytotoxicity

Reduction in CD4/CD8 cell ratio and humoral immune mediator B cells indicates the systemic immune suppression by IONPs. Therefore, next we study the effect of IONPs on regulation of innate immune response using NK-cell against YAC-1 cells. IONPs augmented cytotoxic activity of NK cells at all investigated effector-to-target ratios (200 : 1, 100 : 1, 50 : 1, 25 : 1) (Fig. 6(e)). The NK cell activity was decreased by 41.17% ± 11.74, 69.13 ± 25.07 against untreated control (25 : 1) at 15 and 30 mg kg^{-1} respectively, however response was only significant at 30 mg kg^{-1}. IONPs treatment also reduces the NK cell cytotoxicity. This makes organism vulnerable to opportunistic pathogens, cancer, and other immune related complications.[41]
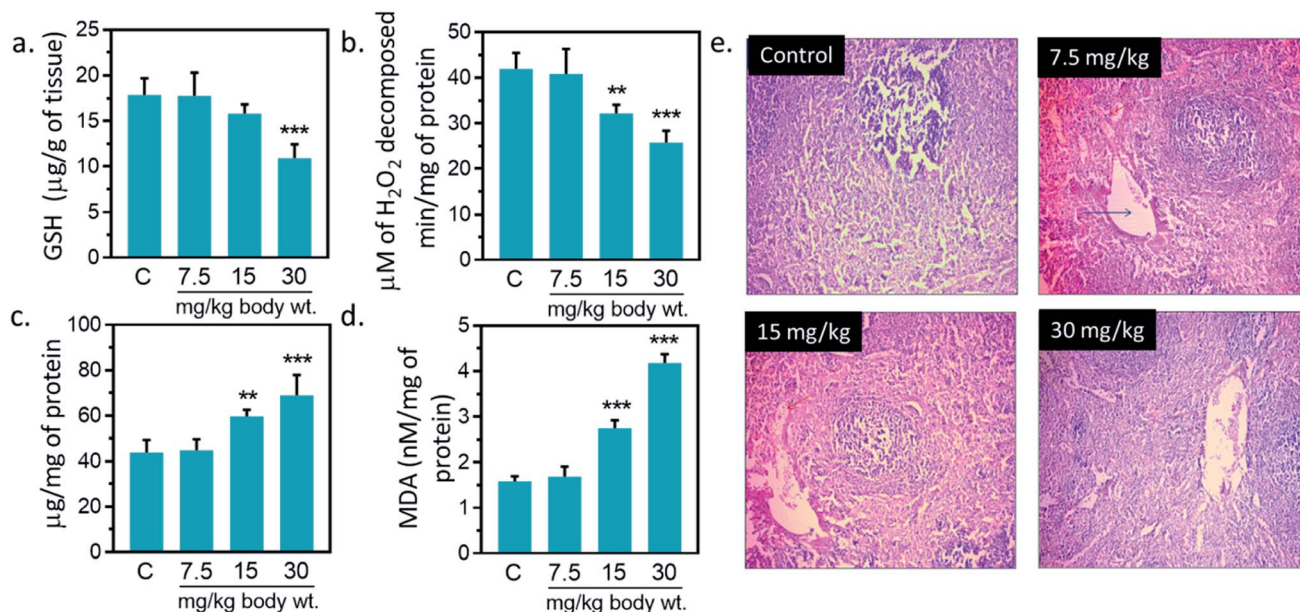
Fig. 7 Effect of Iron oxide nanoparticles (IONPs) on anti-oxidative enzyme level in spleen and spleen architecture. (a) GSH content; (b) catalase activity; (c) superoxide dismutase activity; (d) MDA level; (e) Haematoxylin–eosin staining of spleen sections for seeing the IONPs intoxication. Each data point represents mean ± SD. n: 6. Photomicrograph represents the one of 6-independent experiment. Rats were treated with IONPs intravenously for 28 days in a 7 day interval. *$p < 0.05$; **$p < 0.01$; and ***$p < 0.001$ *versus* saline control.

The increase in B cells indicates the enhancement in humoral immune component.

3.12. Effect of IONPs on antioxidant system of spleen

Antioxidant enzymes act as main line of defense against free radicals in animal.[1,16,17] It catalyzes reactions to neutralize free radicals. SOD detoxifies free radical by catalyzing the dismutation of the superoxide radical into H_2O_2, which subsequently broken into H_2O and O_2 by catalase.[2,16,42] Catalase activity was reduced by 23.1, 38.4% against untreated control at 15, and 30 mg kg^{-1}, respectively (Fig. 7(b)). A significantly increased ($p < 0.05$) in SOD activity was observed at 15, and 30 mg kg^{-1} IONPs against untreated control (Fig. 7(c)). In the present study, IONPs treatment resulted in increased activity of SOD in spleen. Elevated SOD level indicates the presence of oxidative stress in the cells. It also indicates the higher formation rate of intracellular H_2O_2. Earlier, polyethylene glycol-8000 coated superparamagnetic IONPs had showed to increase the SOD activity in liver of Wistar rat liver.[13] A significantly reduction in catalase activity was observed in spleen of all treated group. The reduction in catalase activity may be related to the increase in $O_2^{-\bullet}$ production.[43] Dose dependent reduction in GSH level was observed in IONPs treated rats. GSH level was decreased by 39.13% ± 5.51 ($p < 0.05$) against untreated control at 30 mg kg^{-1} (Fig. 7(a)). Decreased GSH content has been observed in spleen of rats treated with IONPs. The increase in spleen SOD activity suggests the higher formation rate of H_2O_2. Other than catalase, H_2O_2 can be also decomposed by glutathione peroxidase. However, glutathione peroxidase requires GSH for catalytic cycle and lower glutathione suggest the accumulation of H_2O_2 in spleen.[43] In spleen, MDA level was

significantly ($p < 0.05$) elevated by 6, 73.2 and 163.1% against untreated control at 7.5, 15, and 30 mg kg^{-1} IONPs respectively (Fig. 7(a)). Increased MDA level demonstrates that anti-oxidant level was not sufficient to combat the oxidative stress induced by IONPs.[1]

3.13. Histopathological changes due to iron oxide nanoparticles

IONPs accumulation in spleen did not cause any major structural changes in spleen from untreated control as clearly seen in Fig. 7(e) however, slight variations in cell size of spleen was observed at 30 mg per kg dose. Overall, we observed little damage *in vivo* after IONPs treatment. Following these observations, we ought to investigate if accumulation and residence of these nanoparticles within the spleen cause any corrosion on spleen. H&E staining did not show toxicity; however, slight variations in cell content and morphology within the spleen were observed at 30 mg per kg dose. Overall, we observed little or no damage in *in vivo* after IONPs treatment.

4. Conclusion

In present study, we observed minimal to moderate toxic effects of intravenously administered IONPs to rodents. IONPs reduce BM-MNCs proliferation, induces oxidative stress and cell death. IONPs induce immunosuppression represented by reduced NK cells cytotoxicity and lower CD4+/CD8+ ratio. However, it enhances the B cell proportion. IONPs induce inflammatory response, represented by increased pro-inflammatory cytokines (Interleukin (IL)-1β, TNF-α, and IL-6) in serum. Increase in inflammatory response possibly mediated by IONPs activated

M1 macrophage. IONPs exposure also increases lipid peroxidation, and reduces intracellular glutathione and catalase in spleen. Superoxide dismutase level was found to increase in spleen after IONPs treatment. On histological examination, IONPs treatment did not showed any significant injury or structural alteration in spleen at administered dose. Overall, our results suggest that IONPs may cause oxidative stress and cell death by inducing the inflammatory response through M1 macrophage in biological system.

Conflicts of interest

There are no conflicts to declare.

Acknowledgements

References

1 U. S. Gaharwar, R. Meena and P. Rajamani, Iron oxide nanoparticles induced cytotoxicity, oxidative stress and DNA damage in lymphocytes, *J. Appl. Toxicol.*, 2017, **37**(10), 1232–1244.

2 Q. Feng, Y. Liu, J. Huang, K. Chen, J. Huang and K. Xiao, Uptake, distribution, clearance, and toxicity of iron oxide nanoparticles with different sizes and coatings, *Sci. Rep.*, 2018, **8**(1), 1–3.

3 E. Alphandéry, Biodistribution and targeting properties of iron oxide nanoparticles for treatments of cancer and iron anemia disease, *Nanotoxicology*, 2019, **13**(5), 573–596.

4 U. S. Gaharwar, R. Meena and P. Rajamani, Biodistribution, Clearance and Morphological Alterations of Intravenously Administered Iron Oxide Nanoparticles in Male Wistar Rats, *Int. J. Nanomed.*, 2019, **14**, 9677.

5 N. Singh, G. J. Jenkins, R. Asadi and S. H. Doak, Potential toxicity of superparamagnetic iron oxide nanoparticles (SPION), *Nano Rev.*, 2010, **1**(1), 5358.

6 D. Askri, V. Cunin, D. Béal, S. Berthier, B. Chovelon, J. Arnaud, W. Rachidi, M. Sakly, S. Amara, M. Sève and S. G. Lehmann, Investigating the toxic effects induced by iron oxide nanoparticles on neuroblastoma cell line: an integrative study combining cytotoxic, genotoxic and proteomic tools, *Nanotoxicology*, 2019, **13**(8), 1021–1040.

7 V. Kononenko, A. Erman, T. Petan, I. Križaj, S. Kralj, D. Makovec and D. Drobne, Harmful at non-cytotoxic concentrations: SiO2-SPIONs affect surfactant metabolism and lamellar body biogenesis in A549 human alveolar epithelial cells, *Nanotoxicology*, 2017, **11**(3), 419–429.

8 B. Szalay, E. Tátrai, G. Nyírő, T. Vezér and G. Dura, Potential toxic effects of iron oxide nanoparticles in in vivo and in vitro experiments, *J. Appl. Toxicol.*, 2012, **32**(6), 446–453.

9 V. Valdiglesias, N. Fernández-Bertólez, G. Kiliç, C. Costa, S. Costa, S. Fraga, M. J. Bessa, E. Pásaro, J. P. Teixeira and B. Laffon, Are iron oxide nanoparticles safe? Current knowledge and future perspectives, *J. Trace Elem. Med. Biol.*, 2016, **38**, 53–63.

10 Å. Gustafsson, U. Bergström, L. Ågren, L. Österlund, T. Sandström and A. Bucht, Differential cellular responses in healthy mice and in mice with established airway inflammation when exposed to hematite nanoparticles, *Toxicol. Appl. Pharmacol.*, 2015, **288**(1), 1.

11 S. Kumar, R. Meena and R. Paulraj, Role of macrophage (M1 and M2) in titanium-dioxide nanoparticle-induced oxidative stress and inflammatory response in rat, *Appl. Biochem. Biotechnol.*, 2016, **180**(7), 1257–1275.

12 H. Arami, A. Khandhar, D. Liggitt and K. M. Krishnan, In vivo delivery, pharmacokinetics, biodistribution and toxicity of iron oxide nanoparticles, *Chem. Soc. Rev.*, 2015, **44**(23), 8576–8607.

13 B. Rajan, S. Sathish, S. Balakumar and T. Devaki, Synthesis and dose interval dependent hepatotoxicity evaluation of intravenously administered polyethylene glycol-8000 coated ultra-small superparamagnetic iron oxide nanoparticle on Wistar rats, *Environ. Toxicol. Pharmacol.*, 2015, **39**(2), 727–735.

14 R. Riasat and G. Nie, Synthesis and Characterization of Nontoxic Hollow Iron Oxide (-) Nanoparticles Using a Simple Hydrothermal Strategy, *J. Nanomater.*, 2016, **2016**, 1–7.

15 H. Zhang, J. Li, Y. Hu, M. Shen, X. Shi and G. Zhang, Folic acid-targeted iron oxide nanoparticles as contrast agents for magnetic resonance imaging of human ovarian cancer, *J. Ovarian Res.*, 2016, **9**(1), 19.

16 U. S. Gaharwar and R. Paulraj, Iron oxide nanoparticles induced oxidative damage in peripheral blood cells of rat, *J. Biomed. Sci. Eng.*, 2015, **8**(04), 274.

17 S. Kumar and A. B. Tiku, Biochemical and molecular mechanisms of radioprotective effects of naringenin, a phytochemical from citrus fruits, *J. Agric. Food Chem.*, 2016, **64**(8), 1676–1685.

18 K. Kavithaa, M. Paulpandi, P. R. Padma and S. Sumathi, Induction of intrinsic apoptotic pathway and cell cycle arrest via baicalein loaded iron oxide nanoparticles as a competent nano-mediated system for triple negative breast cancer therapy, *RSC Adv.*, 2016, **6**(69), 64531–64543.

19 S. Kumar, R. Meena and P. Rajamani, Fabrication of BSA–green tea polyphenols–chitosan nanoparticles and their role in radioprotection: a molecular and biochemical approach, *J. Agric. Food Chem.*, 2016, **64**(30), 6024–6034.

20 R. Varshney and R. K. Kale, Effects of calmodulin antagonists on radiation-induced lipid peroxidation in microsomes, *Int. J. Radiat. Biol.*, 1990, **58**(5), 733–743.

21 S. Marklund and G. Marklund, Involvement of the superoxide anion radical in the autoxidation of pyrogallol and a convenient assay for superoxide dismutase, *Eur. J. Biochem.*, 1974, **47**(3), 469–474.

22 H. Aebi, Catalase in vitro, *Methods Enzymol.*, 1984, **105**, 121–126.

23 A. O. Dada, F. A. Adekola, E. O. Odebunmi, F. E. Dada, O. S. Bello and A. S. Ogunlaja, Bottom-up approach synthesis of core-shell nanoscale zerovalent iron (CS-nZVI): physicochemical and spectroscopic characterization with Cu (II) ions adsorption application, *MethodsX*, 2020, **7**, 100976.

24 A. O. Dada, F. A. Adekola and E. O. Odebunmi, Kinetics, mechanism, isotherm and thermodynamic studies of liquid phase adsorption of Pb2+ onto wood activated carbon supported zerovalent iron (WAC-ZVI) nanocomposite, *Cogent Chem.*, 2017, **3**(1), 1351653.

25 Y. Chen, J. Li, Z. Yuan, J. Feng and Z. Chen, Metabolic fate and subchronic biological effects of core–shell structured Fe3O4@ SiO2-NH2 nanoparticles, *Nanotoxicology*, 2018, **12**(6), 621–636.

26 L. Kautz and E. Nemeth, Molecular liaisons between erythropoiesis and iron metabolism. Blood, *Journal of the American Society of Hematology*, 2014, **124**(4), 479–482.

27 S. J. Soenen and M. De Cuyper, Assessing cytotoxicity of (iron oxide-based) nanoparticles: an overview of different methods exemplified with cationic magnetoliposomes, *Contrast Media Mol. Imaging*, 2009, **4**(5), 207–219.

28 R. J. Wydra, C. E. Oliver, K. W. Anderson, T. D. Dziubla and J. Z. Hilt, Accelerated generation of free radicals by iron oxide nanoparticles in the presence of an alternating magnetic field, *RSC Adv.*, 2015, **5**(24), 18888–18893.

29 Z. Yarjanli, K. Ghaedi, A. Esmaeili, S. Rahgozar and A. Zarrabi, Iron oxide nanoparticles may damage to the neural tissue through iron accumulation, oxidative stress, and protein aggregation, *BMC Neurosci.*, 2017, **18**(1), 51.

30 C. Peng, Y. Chen, Y. Shan, H. Zhang, Z. Guo, D. Li and S. Li, LSK Derived LSK–Cells Have a High Apoptotic Rate Related to Survival Regulation of Hematopoietic and Leukemic Stem Cells, *PLoS One*, 2012, **7**(6), 1–11.

31 S. Sruthi, L. Maurizi, T. Nury, F. Sallem, J. Boudon, J. M. Riedinger, N. Millot, F. Bouyer and G. Lizard, Cellular interactions of functionalized superparamagnetic iron oxide nanoparticles on oligodendrocytes without detrimental side effects: cell death induction, oxidative stress and inflammation, *Colloids Surf., B*, 2018, **170**, 454–462.

32 Z. Huang, B. Xu, X. Huang, Y. Zhang, M. Yu, X. Han, L. Song, Y. Xia, Z. Zhou, X. Wang and M. Chen, Metabolomics reveals the role of acetyl-l-carnitine metabolism in γ-Fe2O3 NP-induced embryonic development toxicity via mitochondria damage, *Nanotoxicology*, 2019, **13**(2), 204–220.

33 Y. H. Luo, L. W. Chang and P. Lin, Metal-based nanoparticles and the immune system: activation, inflammation, and potential applications, *BioMed Res. Int.*, 2015, **2015**, 1–12.

34 C. He, S. Jiang, H. Yao, L. Zhang, C. Yang, D. Zhan, G. Lin, Y. Zeng, Y. Xia, Z. Lin and G. Liu, Endoplasmic reticulum stress mediates inflammatory response triggered by ultra-small superparamagnetic iron oxide nanoparticles in hepatocytes, *Nanotoxicology*, 2018, **12**(10), 1198–1214.

35 A. Shah and M. A. Dobrovolskaia, Immunological effects of iron oxide nanoparticles and iron-based complex drug formulations: therapeutic benefits, toxicity, mechanistic insights, and translational considerations, *Nanomedicine*, 2018, **14**(3), 977–990.

36 C. Figueiredo Borgognoni, J. H. Kim, V. Zucolotto, H. Fuchs and K. Riehemann, Human macrophage responses to metal-oxide nanoparticles: a review, *Artif. Cells, Nanomed., Biotechnol.*, 2018, **46**(2), 694–703.

37 J. M. Rojas, L. Sanz-Ortega, V. Mulens-Arias, L. Gutiérrez, S. Pérez-Yagüe and D. F. Barber, Superparamagnetic iron oxide nanoparticle uptake alters M2 macrophage phenotype, iron metabolism, migration and invasion, *Nanomedicine*, 2016, **12**(4), 1127–1138.

38 X. Yang, Y. Zhang, W. Lai, Z. Xiang, B. Tu, D. Li, X. Nan, C. Chen, Z. Hu and Q. Fang, Proteomic profiling of RAW264. 7 macrophage cells exposed to graphene oxide: insights into acute cellular responses, *Nanotoxicology*, 2019, **13**(1), 35–49.

39 S. Xiong, H. She and H. Tsukamoto, Signaling role of iron in NF-kappa B activation in hepatic macrophages, *Comp. Hepatol.*, 2004, **3**(1), S36.

40 R. E. Mebius and G. Kraal, Structure and function of the spleen, *Nat. Rev. Immunol.*, 2005, **5**(8), 606–616.

41 V. Patsula, J. Tulinska, Š. Trachtová, M. Kuricova, A. Liskova, A. Španová, F. Ciampor, I. Vavra, B. Rittich, M. Ursinyova and M. Dusinska, Toxicity evaluation of monodisperse PEGylated magnetic nanoparticles for nanomedicine, *Nanotoxicology*, 2019, **13**(4), 510–526.

42 S. Kumar, R. K. Singh and R. Meena, Emerging targets for radioprotection and radiosensitization in radiotherapy, *Tumor Biol.*, 2016, **37**(9), 11589–11609.

43 A. C. Bainy, E. Saito, P. S. Carvalho and V. B. Junqueira, Oxidative stress in gill, erythrocytes, liver and kidney of Nile tilapia (Oreochromis niloticus) from a polluted site, *Aquat. Toxicol.*, 1996, **34**(2), 151–162.